

AD A049340

Annual Report

Covering the Period June 1, 1976 through September 30, 1977

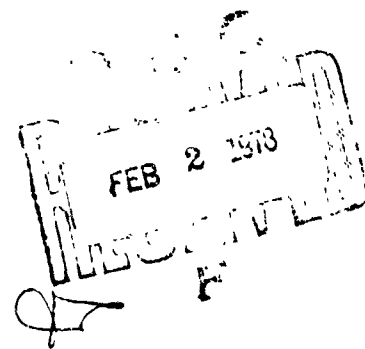
**STUDIES OF HOMOGENEOUS AND
HETEROGENEOUS HYDRAZINE DECOMPOSITION
FOR MONOPROPELLANT PROPULSION SYSTEMS**

By: A. C. BALDWIN, D M GOLDEN, K E LEWIS,
R T. REWICK, and H WISE

Prepared for

AIR FORCE OFFICE OF SCIENTIFIC RESEARCH
1400 WILSON BOULEVARD
ARLINGTON, VIRGINIA 22209

AFOSR CONTRACT F44620-73-C-0069



STANFORD RESEARCH INSTITUTE
Menlo Park, California 94025 · U.S.A.

SECURITY CLASSIFICATION OF THIS PAGE (When Data Entered)

REPORT DOCUMENTATION PAGE		READ INSTRUCTIONS BEFORE COMPLETING FORM
1. REPORT NUMBER AFOSR-TR- 77 - 1301 ✓	2. GOVT ACQUISITION NO.	3. RECIPIENT'S CATALOG NUMBER
4. TITLE (and Subtitle) STUDIES OF HOMOGENEOUS AND HETEROGENEOUS HYDRAZINE DECOMPOSITION FOR MONOPROPELLANT PROPULSION SYSTEMS ✓	5. TYPE OF REPORT & PERIOD COVERED FINAL 1 June 1976 -30 Sep 77.	
7. AUTHOR(s) A C BALDWIN R T REWICK D M GOLDEN H WISE K E LEWIS	6. PERFORMING ORG. REPORT NUMBER	
9. PERFORMING ORGANIZATION NAME AND ADDRESS STANFORD RESEARCH INSTITUTE ✓ MENLO PARK, CALIFORNIA 94025	8. CONTRACT OR GRANT NUMBER(s) ✓ F44620-73-C-0069	
11. CONTROLLING OFFICE NAME AND ADDRESS AIR FORCE OFFICE OF SCIENTIFIC RESEARCH/NA BLDG 410 BOLLING AIR FORCE BASE, D C 20332	10. PROGRAM ELEMENT, PROJECT, TASK AREA & WORK UNIT NUMBERS 2308A1 61102F	
14. MONITORING AGENCY NAME & ADDRESS (if different from Controlling Office)	12. REPORT DATE Oct 77	
	13. NUMBER OF PAGES 46	
	15. SECURITY CLASS. (of this report) UNCLASSIFIED	
	15a. DECLASSIFICATION/DOWNGRADING SCHEDULE	
16. DISTRIBUTION STATEMENT (of this Report) Approved for public release; distribution unlimited.		
17. DISTRIBUTION STATEMENT (of the abstract entered in Block 20, if different from Report)		
18. SUPPLEMENTARY NOTES		
19. KEY WORDS (Continue on reverse side if necessary and identify by block number) HYDRAZINE MONOPROPELLANTS SPACE PROPULSION		
20. ABSTRACT (Continue on reverse side if necessary and identify by block number) The properties of alumina-supported Ir-Ni alloy catalysts for the decomposition of hydrazine have been examined over a range of mixed-metal compositions. The results demonstrate that the addition of Ni to Ir increases the specific catalyt- ic activity, with a maximum at 35 atomic percent Ni, and at the same time reduces the decay in activity caused by the accumulation of reaction products over a range of Ni-Ir alloy compositions. ↗		



STANFORD RESEARCH INSTITUTE
Menlo Park, California 94025 · U.S.A.

Annual Report

Covering the Period June 1, 1976 through September 30, 1977

11

31

October 1977

1248p.

6

**STUDIES OF HOMOGENEOUS AND
HETEROGENEOUS HYDRAZINE DECOMPOSITION
FOR MONOPROPELLANT PROPULSION SYSTEMS •**

Final rept. 2 11-76-34 of 77

10

By A C BALDWIN, D M GOLDEN, K E LEWIS,
R T REWICK, and H WISE

Prepared for:

AIR FORCE OFFICE OF SCIENTIFIC RESEARCH
1400 WILSON BOULEVARD
ARLINGTON, VIRGINIA 22209

15

AFOSR CONTRACT F44620-73-C-0089

SRI Project PYU-2716

1223081

Approved by:

MARION E. HILL, Director
Chemistry Laboratory

17A11

P J JORGENSEN, Vice President
Life and Physical Sciences

AIR FORCE OFFICE OF SCIENTIFIC RESEARCH (AFOSR)
1400 WILSON BOULEVARD
ARLINGTON, VIRGINIA 22209

1 and 15
100-23 (7b).

CONTENTS

PREFACE	1
 <u>Section 1:</u> CATALYTIC PROPERTIES OF Al_2O_3 SUPPORTED Ir AND Ir-Ni ALLOY CRYSTALLITES FOR HYDRAZINE DECOMPOSITION	
ABSTRACT	3
I. INTRODUCTION	4
II. EXPERIMENTAL DETAILS	5
A. Catalyst Preparation	5
B. Apparatus	5
C. Physical Properties	6
III. RESULTS	7
A. Composition of Alloy Catalyst	7
B. CO Adsorption	7
C. Catalytic Activity for Hydrazine Decomposition	7
D. Catalyst Deactivation	10
E. Pulse Shape Analysis	10
IV. DISCUSSION	14
 <u>Section 2:</u> DECOMPOSITION KINETICS OF N_2H_4 CATALYZED BY ALUMINA-SUPPORTED IRIDIUM	
ABSTRACT	15
I. INTRODUCTION	16
II. EXPERIMENTAL DETAILS	17
III. RESULTS	18
A. Experimental Influences on Catalyst Activity	18
B. Experiments Using Pelletized Catalyst	19
C. Experiments Using Powdered Catalyst	19
D. Products of the Reaction	26
IV. DISCUSSION	30
REFERENCES	33
APPENDIX	34

ILLUSTRATIONS

1. X-Ray Diffraction Data for Al_2O_3 -Supported Ir-Ni System .	8
2. Activity Pattern of Ni-Ir/ Al_2O_3 Catalyst for Hydrazine Decomposition	11
3. Plot of Log (Concentration of Hydrazine Decomposed) Against Log (Concentration of Hydrazine Remaining).	20
4. Plot of Log (Concentration of Hydrazine Decomposed) Against Log (Concentration of Hydrazine Remaining).	21
5. Plot of Log (Concentration of Hydrazine Decomposed) Against Log (Concentration of Hydrazine Remaining).	22
6. Plot of Log (Concentration of Hydrazine Decomposed) Against Log (Concentration of Hydrazine Remaining).	24
7. Plot of Log (Concentration of Hydrazine Decomposed) Against Log (Concentration of Hydrazine Remaining).	25
8. Arrhenius Plot of the Decomposition of Hydrazine on Powdered Catalyst.	27
9. Arrhenius Plot of the Decomposition of Hydrazine on Powdered Catalyst.	28
10. Product Distribution as a Function of Temperature	29

TABLES

I	CO Adsorption Studies with [Ni-Ir]/Al ₂ O ₃ Catalysts at 300 K	9
II	Activity of Ir/Al ₂ O ₃ and [Ni-Ir]/Al ₂ O ₃ Catalysts for N ₂ H ₄ Decomposition at 300 K	9
III	Catalyst Deactivation by Prolonged Exposure to Hydrazine	12
IV	Pulse Shape Analysis of Nitrogen Product Transient from N ₂ H ₄ Pulse	12
A-1	Data for Figure 6	35
A-2	Data for Figure 7	37
A-3	Data for Figure 8	38
A-4	Data for Figure 9	40
A-5	Data for Figure 10	42

PREFACE

Considerable effort has been devoted to developing a N_2H_4 fueled monopropellant control thruster capable of reliable and prolonged operation in a space environment. Current monopropellant engines use a Shell-405 catalyst bed (an alumina-supported iridium catalyst) to decompose liquid hydrazine into hot gaseous products. However, during repetitive operation of such engines in a limited pulse mode cycle, the catalytic reactor exhibits a gradual loss of thrust attributable to a deterioration in catalyst performance. Ultimately "washout" occurs; a process in which liquid N_2H_4 penetrates through the catalyst bed without decomposition.

The mechanism of catalyst-activity loss is not established unequivocally. However, two processes are known to occur. One involves the physical breakup of the catalyst caused by either thermal shocks over the large temperature range experienced during operation, or large pressure gradients generated within the catalyst particle resulting from pore wetting by liquid reactant. The other cause of catalyst deactivation is to be found in catalyst surface poisoning, i.e., the irreversible formation of surface species strongly bound to a significant part of the catalyst surface. Our earlier studies with polycrystalline Ir and alumina-supported Ir (Shell-405) identified the presence of hydrogen and nitrogen adatoms with several distinct binding-energy states on the surface of the metal. The results suggested that strongly bound nitrogen adspecies formed during N_2H_4 decomposition can contribute to the loss of catalyst activity encountered during N_2H_4 exposure, especially at catalyst temperatures below 500 K.

To remedy this problem indigenous to the Ir-N₃H₄ system, we examined the feasibility of modifying the binding energy of surface adsorbates by forming a two-component alloy with Ir. The results of this work involving an alumina-supported Ir-Ni alloy catalyst are described in the first section of this report. Section 2 describes the experimental work on N₂H₄ decomposition kinetics catalyzed by Ir/Al₂O₃.

Section 1

CATALYTIC PROPERTIES OF Al_2O_3 SUPPORTED Ir AND Ir-Ni ALLOY CRYSTALLITES FOR HYDRAZINE DECOMPOSITION -

R. T. Rewick and H. Wise

ABSTRACT

The properties of alumina-supported Ir-Ni alloy catalysts for the decomposition of hydrazine have been examined over a range of mixed-metal compositions. The results demonstrate that the addition of Ni to Ir increases the specific catalytic activity, with a maximum at 35 atomic percent Ni, and at the same time, reduces the decay in activity caused by the accumulation of reaction products over a range of Ni-Ir alloy compositions.

I. INTRODUCTION

In a study aimed at reducing the long-term performance decay of Shell-405 catalyst ($\text{Ir}/\text{Al}_2\text{O}_3$) in attitude control thruster operation with N_2H_4 monopropellant, we have examined the beneficial effects provided by transition-metal promoted $\text{Ir}/\text{Al}_2\text{O}_3$ catalysts. Based on the observation that catalyst decay is caused in part by the formation of strongly bound nitrogen adspecies that are intermediate products of hydrazine decomposition,^{1,2} we selected the concept of metal-alloy formation to modify the binding energy of adsorbates. It is known that for certain reaction the catalytic properties of group VIII metals can be altered by alloy formation with another metal component. Recent photoemission studies with two-component systems have provided some information on the changes in electronic properties brought about by alloy formation. Combined with thermal desorption data, these results have given some insight into the local nature of chemical surface bonding and its modification by substrate alloying.

For our studies of Ir-alloy catalysis we selected the homogeneous, random alloy system formed by admixture of nickel to iridium.³ In the measurements performed in this study, we compared the properties of the alumina-supported mixed metal system with those of $\text{Ir}/\text{Al}_2\text{O}_3$ (Shell-405) in terms of hydrazine decomposition rates and surface poisoning by reaction products.

II. EXPERIMENTAL DETAILS

A. Catalyst Preparation

The nickel-promoted catalyst was prepared by impregnating the Ir/Al₂O₃ catalyst (Shell-405) with an aqueous solution of Ni(NO₃)₂·6H₂O. To attain the desired weight loading of metallic Ni, we adjusted the concentration of the nickel salt in the aqueous solution to a specific value and allowed a measured aliquot of the solution to wet the Al₂O₃ supported iridium catalyst (10 wt% Ir). The mixture was evaporated to dryness on a steam bath, air dried at 573 K, and calcined for 1 hour at 573 K. The sample was reduced in H₂ (1 atm) for several hours at 723 K followed by heat treatment in He at 723 K for 15 hours. The nickel weight loadings prepared ranged from 2 to 10 wt% on a dried and reduced basis.

B. Physical Properties

Alloy formation of the Al₂O₃-supported mixed-metal catalyst (Ir-Ni) was followed by x-ray diffraction measurements after H₂ reduction and heating in He at elevated temperature.

C. Apparatus

A powdered sample of catalyst (1.5 ± 0.3 mg) was placed on the glass frit of a differential flow Pyrex microreactor. By use of Loenco switching valves, the reactor could be operated in either of two modes. In the reduction mode, the catalyst was exposed in situ to a stream of H₂ (723 K, 1 hour) and then flushed in He (723 K, 1/2 hour). In the reaction mode, the catalyst was exposed to a N₂H₄ reactant stream

(about 2 vol% N_2H_4 , 98 vol% He) generated by bubbling He at a slow rate through liquid N_2H_4 (Olin technical grade). After a specified time of exposure to gaseous N_2H_4 , the catalyst activity was examined at 300 K by injecting an aliquot of liquid N_2H_4 (6.3×10^{-6} mol) through a rubber septum above the reactor into a He carrier stream. The reactant was vaporized before coming in contact with the catalyst by heating the upper inlet section of the reactor. The degree of N_2H_4 conversion was determined by gas chromatographic analysis (gc) of the mass of N_2 formed after removal of unreacted N_2H_4 and NH_3 from the product stream by condensation in a cold trap (77 K). The analysis quantitatively measures catalyst activity, since NH_3 and N_2 are the only products of N_2H_4 decomposition at 300 K.²

Carbon monoxide adsorption was measured by pulsing the catalyst with aliquots of a 10 vol% CO-in-He mixture at 300 K until gc analysis indicated that no more CO was removed from the pulse. These data were used to evaluate the total amount of CO-adsorbate.

All gases used in this study were purified as follows: H_2 was diffused through a Pd thimble at 573 K; He was passed over copper turnings at 523 K and a molecule sieve (Union Carbide 5A) at 77 K; CO/He was passed through a glass bead trap at 77 K.

III. RESULTS

A. Composition of Alloy Catalyst

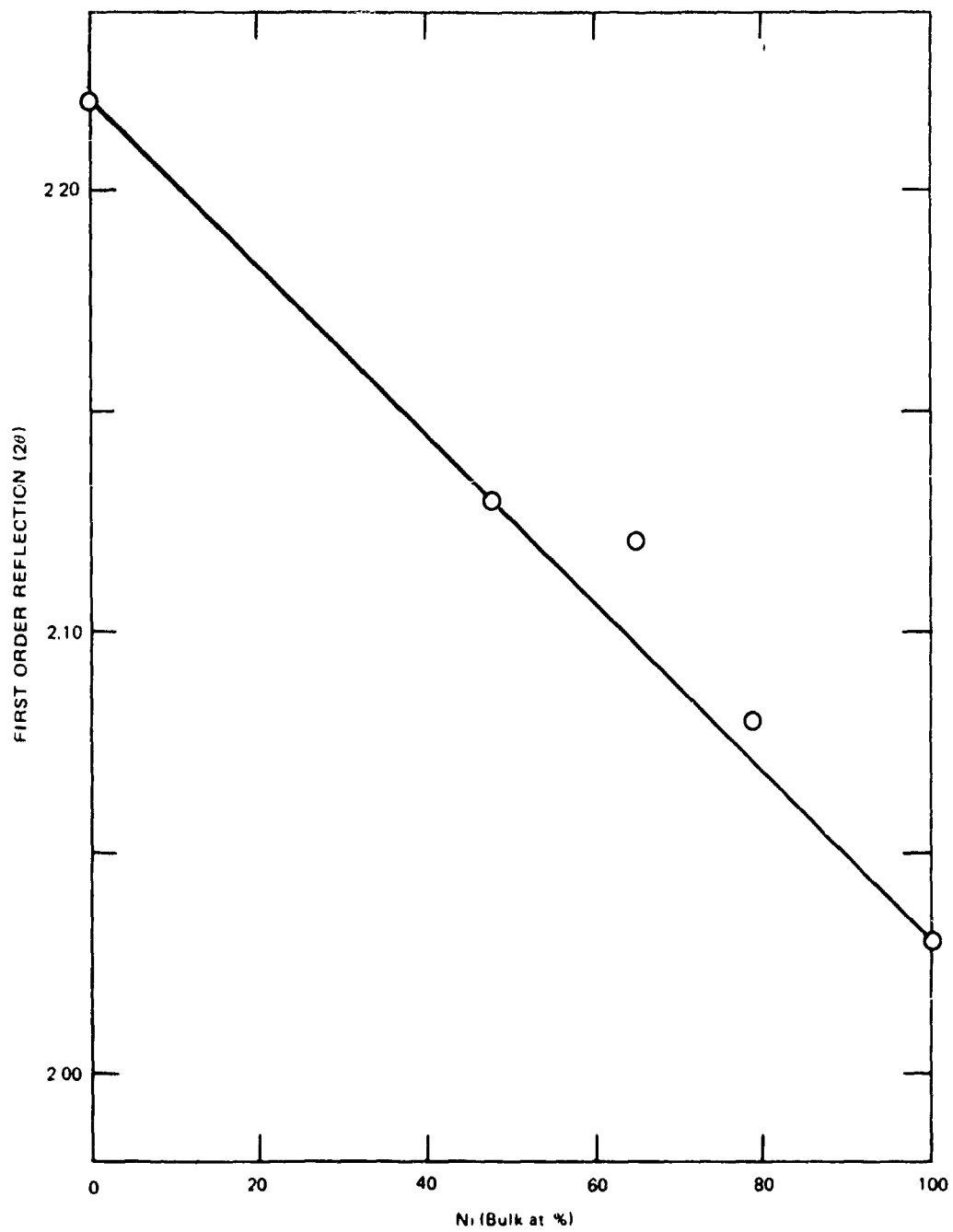
The x-ray diffraction results indicate that the 15-hour heat treatment at 723 K was adequate for alloy formation. The change in interatomic spacing of the fcc two-component lattice, as given by the x-ray diffraction maxima, follows Vegard's law (Figure 1), indicating homogeneous alloy formation.

B. CO Adsorption

The CO adsorption experiment is a measure of the total number of surface sites of the catalyst samples prepared. On the basis of total metal weight loading (Table I), the formation of the dispersed Ir-Ni alloy catalysts decreased slightly the total number of adsorption sites, as reflected by the amount of CO adsorbed at saturation coverage per gram of total metal. However, the changes are relatively small. At a bulk compositions of 21 Ir/79 Ni, the adsorption site density is reduced by less than 30%. In comparing the activities of the catalysts of different metal compositions, it is useful to relate the fractional conversion of N_2H_4 to the total number of metal surface sites available, as determined by CO adsorption.

C. Catalytic Activity for Hydrazine Decomposition

For a first-order surface reaction, such as N_2H_4 decomposition on Ir/ Al_2O_3 , the pulse microreactor technique allows quantitative evaluation of kinetic rate data. Bassett and Habgood⁴ showed that for a first-order reaction, in which the surface reaction rather than the attainment of adsorption equilibrium is rate controlling, the logarithmic fractional



SA 2716 58

FIGURE 1 X-RAY DIFFRACTION DATA FOR Al₂O₃-SUPPORTED Ir-Ni SYSTEM

Table I
CO ADSORPTION STUDIES WITH [Ni-Ir]/Al₂O₃ CATALYSTS AT 300 K

Catalyst Composition (at.%)		Metal Weight Loading (wt%)	Carbon Monoxide Adsorbed	
Ir	Ni		(mol/g catalyst) x 10 ⁴	(mol/g metal) x 10 ³
100 [*]	0	10.0	1.85	1.85
76	24	10.8	1.53	1.42
52	48	12.0	1.79	1.49
35	65	14.8	2.16	1.46
21	79	19.1	2.51	1.31
0	100	10.1	0.50	0.50

* Catalyst prepared by Shell Development Co., (Lab No. 11724-78).

Table II
ACTIVITY OF Ir/Al₂O₃ AND [Ni-Ir]/Al₂O₃ CATALYSTS
FOR N₂H₄ DECOMPOSITION AT 300 K

Catalyst Composition (at.%)		Specific Logarithmic Conversion (mol CO ads) ⁻¹	Fractional Conversion of N ₂ H ₄ Pulse ^a
Ir	Ni		
100	0	378	57
76	24	543	66
52	48	511	77
35	65	310	61
21	79	255	59
0	100	20	6

^a Pulse volume = 6.3 x 10⁻⁶ mol N₂H₄.

conversion of reactant contained in the pulse is proportional to a conversion coefficient, which is the product of the rate constant k , the adsorption equilibrium constant K , and the retention time τ . To make the comparison between the various catalysts meaningful, we have expressed the results in terms of the specific pulse conversion ratio σ (Table II), the ratio of the logarithmic fractional conversion to the total number of metal surface sites of the catalyst, as measured by CO absorption (Table I).

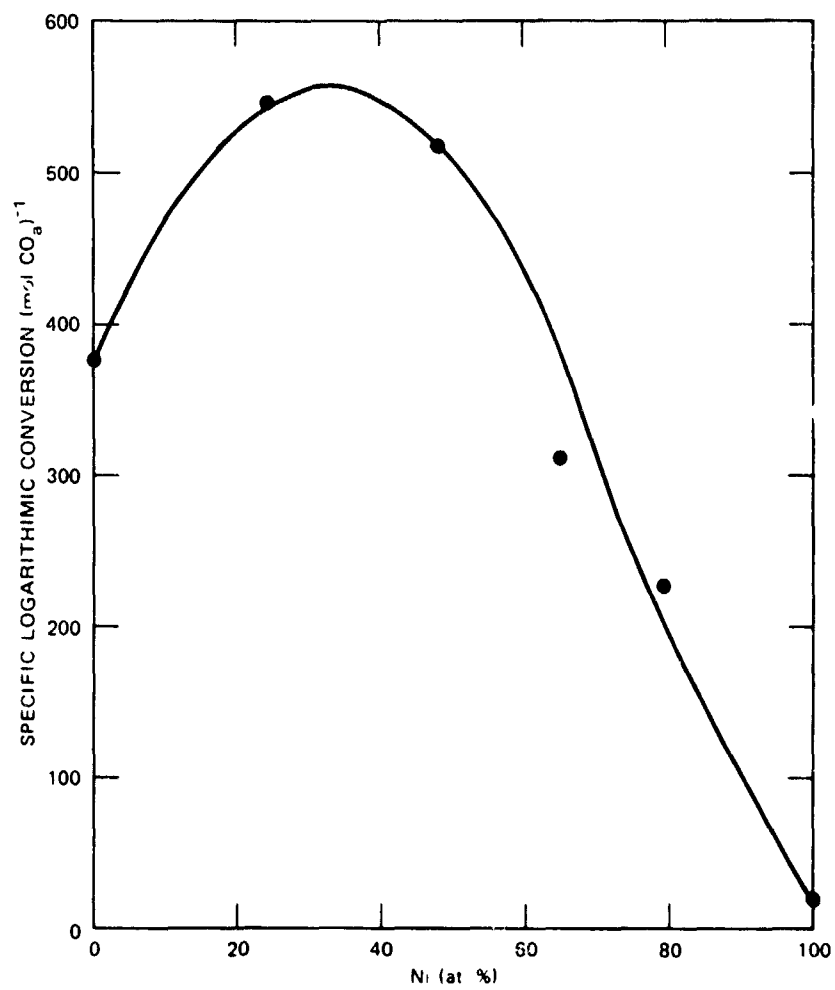
The addition of Ni to the Ir-containing catalyst markedly influences the activity pattern. Rather than a monotonic decrease in N_2H_4 decomposition activity, as may be expected from dilution of the Ir surface sites by nickel atoms, the mixed-metal catalyst system exhibits a pronounced activity maximum at a composition equivalent to 65 Ir/35 Ni (at.%(see Figure 2).

D. Catalyst Deactivation

An important aspect of our study was to examine the process of catalyst deactivation resulting from prolonged exposure of the Ir/ Al_2O_3 and Ir/Ni/ Al_2O_3 catalysts to hydrazine. The degree of deactivation diminishes significantly in the two-component catalyst system (Table III), especially for the catalysts containing more than 25 at.% Ni. Also, the Ni/Ir/ Al_2O_3 catalysts containing 35 at.% Ni offers the advantage of higher specific activity and greater resistance to surface deactivation (Figure 2).

E. Pulse Shape Analysis

Another measure of catalyst performance is the shape of the product pulse transient emerging from the catalytic reactor after injection of the reactant pulse into the carrier gas stream. The pulse shape analysis is restricted to a comparison of the product transients exhibited by



SA 2716-69

FIGURE 2 ACTIVITY PATTERN OF Ni-Ir/Al₂O₃ CATALYST FOR HYDRAZINE DECOMPOSITION

Table III

CATALYST DEACTIVATION BY PROLONGED EXPOSURE TO HYDRAZINE^a

Catalyst Composition (at.%)		Fractional Activity Loss ^b (%)
Ir	Ni	
100	0	52
76	24	53
52	48	29
35	65	27
21	79	32

^a Each catalyst sample exposed continuously to 8.4×10^{-4} mole of N_2H_4 at 448 K before testing for activity with a pulse of N_2H_4 (6.3×10^{-6} mol) at 300 K.

^b Evaluated from logarithmic fractional conversion per gram of total metal of fresh and used catalyst samples.

Table IV

PULSE SHAPE ANALYSIS OF NITROGEN
PRODUCT TRANSIENT FROM N_2H_4 PULSE^a

Catalyst Composition (wt%) Ir	Pulse Shape Parameters ^b			
	Fresh Catalyst		Used Catalyst ^c	
	C/C (Ir)	ϵ/ϵ (Ir)	C/C (Ir)	ϵ/ϵ (Ir)
100	1.0	1.0	1.0	1.0
76	1.3	1.1	0.8	0.8
52	1.6	1.1	2.8	1.2
35	0.7	0.8	1.8	1.0
21	0.4	0.7	1.3	0.9
0	0.2	1.1	---	---

^a N_2H_4 pulse contained 6.3×10^{-6} mol N_2H_4 at 300 K.

^b Relative to Ir/Al_2O_3 .

^c After exposure to 840×10^{-6} mol N_2H_4 at 448 K.

Ir/Al₂O₃ and [Ni-Ir]/Al₂O₃. Parametric analysis of the N₂ product pulse demonstrated that to a first approximation the exit pulse may be described by the function $f(t) = Ct \exp(-\epsilon t)$, where C and ϵ are coefficients associated with the pulse shape and t is time. Large values of C and ϵ indicate a fast rise and decay of the product pulse. We used this analysis to compare the pulse characteristics of the product stream leaving the catalytic reactor at constant conditions of carrier gas flow, temperature, and pressure (Table IV). The observed increase in the C- and ϵ parameters indicates a marked improvement in performance of the fresh alloy catalyst when Ni is added. Examination of the pulse shape of the used catalyst (after exposure to 8.4×10^{-4} mol N₂H₄ at 448 K) revealed little deterioration in catalyst performance for the catalyst with a composition in excess of 40 at.% Ni. Selecting the composition 52 Ir/48 Ni, we observe the following improved catalyst performance when Ni is added to Ir:

- (1) Specific conversion of fresh catalyst has increased
- (2) Retention time by catalyst bed has diminished
- (3) Deactivation by reaction products has decreased.

IV. DISCUSSION

For the catalytic decomposition of N_2H_4 , the mixed metal system $[Ir-Ni]/Al_2O_3$ exhibits significant improvement over Ir/Al_2O_3 in terms of specific conversion and catalyst deactivation. Both parameters relate to changes in bonding of surface intermediates brought about by the presence of Ni and Ir atoms in the alloy. It is unlikely that we are dealing here with a predominantly geometric effect in which the Ir site density is simply diluted by Ni atoms, which exhibit poor catalytic activity (Table II). Such a change in topography would result in the gradual decrease in N_2H_4 conversion, if pairs of nearest or next-nearest Ir atoms were required for initial adsorption.^{1,2} Rather, the results point to an electronic alloy effect in which the binding energy of the reaction intermediate is decreased enough to prevent its accumulation and conversion to an indigenous surface poison. It would be desirable to measure the binding energies of the reaction intermediate on $Ir-Ni/Al_2O_3$ and Ir/Al_2O_3 catalysts by temperature programmed desorption experiments.

In conclusion, this study demonstrates that thermally stable alloy crystallites composed of Ir and Ni can be prepared on an Al_2O_3 support. The catalytic properties of the supported mixed-metal system for N_2H_4 decomposition are superior to those of Ir/Al_2O_3 in terms of specific activity and catalyst life.

Section 2

DECOMPOSITION KINETICS OF N_2H_4 CATALYZED BY ALUMINA-SUPPORTED IRIIDIUM

A. C. Baldwin, K. E. Lewis, and D. M. Golden

ABSTRACT

The kinetics of the decomposition of hydrazine on Shell-405 catalyst have been investigated at low pressures between 300 and 900 K. The catalyst treatment was found to have a profound effect on the measured rate of decomposition.

I. INTRODUCTION

Current monopropellant attitude control thrusters using Shell-405 catalyst ($\text{Ir}/\text{Al}_2\text{O}_3$) and hydrazine fuel exhibit a long-term performance decay due to catalyst poisoning. To understand this effect, we have investigated the kinetics of the decomposition at low pressures on unpoisoned catalyst from 300 to 900 K. This established a baseline of reactivity to which work on the mechanism of poisoning could be related.

We have measured the rate of decomposition of hydrazine as a function of temperature, pressure (concentration of reactant), catalyst particle size, and catalyst pretreatment. Both the catalyst pretreatment and the history of the catalyst between pretreatment and commencing the measurements were found to have a crucial effect on the measured rate of decomposition. This behavior has inhibited our attempts to completely understand the kinetics of hydrazine decomposition. Previously reported work is reviewed and discussed in the light of these newly discovered experimental problems.

II. EXPERIMENTAL DETAILS

The measurements were carried out in a very low-pressure pyrolysis (VLPP) system that has been fully described.^{7,8} Briefly, the system consists of a Knudsen cell reactor into which gas molecules flow at a rate of $\sim 10^{15} - 10^{17}$ molec. s^{-1} . While in the reactor, the molecules collide principally with the walls and catalyst, if present, but not with each other. The molecules leave the reactor through an aperture at a known rate, relative to which the rate of any chemical reaction occurring may be measured. This aperture may have two sizes (1-mm and 3-mm diameter), which, for a given flow of gas, varies the pressure in the reactor by a factor of 9. When the aperture size as well as the reactant flow rate is varied, a wide range of pressures (concentrations) in the reactor is easily achieved. The effusing reactants and products are formed into a molecular beam and are detected and measured using a phase-sensitive quadrupole mass spectrometer.

The catalyst was heated to 1000 K under vacuum ($\sim 10^{-8}$ torr), pulsed with large concentrations of hydrogen, heated again at 1000 K under vacuum, and then cooled under vacuum. The catalyst used was Shell-405 (32% Ir on Al_2O_3) batch. Two types of hydrazine were used--normal technical grade and a specially purified sample that contained no impurities detectable by analytical mass spectrometry. This latter sample was not exposed to the atmosphere at any time before use.

III. RESULTS

A. Experimental Influences on Catalyst Activity

We have found that technical grade hydrazine gives identical results to pure vacuum-handled samples in terms of rate of decomposition and rate of initial poisoning. These results agree with previous work⁷ in which hydrazine containing 5% water was found to give identical results to dry hydrazine. We have not investigated long-term poisoning effects.

Measurement of the rates of decomposition of hydrazine shows that several factors have a profound effect on the catalyst activity. In periods as short as 4 hours, the activity of the catalyst declines measurably when the catalyst is left under high vacuum ($\sim 10^{-8}$ torr) at room temperature. During catalyst activation, the time of heating at 1000 K after reaction with hydrogen markedly changed the initial measured activity. In general, at least 30 minutes at this temperature was required to achieve maximum activity. However, the activation process was largely irreproducible. For instance, a given catalyst sample subjected to the same activation treatment on 2 consecutive days yielded rates of initial decomposition of hydrazine that differed by a factor of 3. Since the catalyst must be activated before each experiment due to the "vacuum-poisoning" effect noted above, the irreproducibility of the activation process makes it difficult to compare experimental results.

A similar problem was encountered when we conducted experiments at different temperatures. If the catalyst was activated at 1000 K and then cooled to 500 K under vacuum ($\sim 10^{-8}$ torr), a different activity was observed than when the catalyst was cooled to room temperature and then heated to 500 K. Thus, it seems some deactivation may occur during the

cooling process in the reaction chamber, and experiments conducted at different temperatures may reflect a variable deactivation due to the time taken to reach that temperature from 1000 K.

B. Experiments Using Pelletized Catalyst

We first investigated the rate of reaction on five normal pellets of Shell-405 in the temperature range 300 to 600 K. This is the temperature range over which catalyst poisoning was previously found to occur.⁷ The results at 408, 472, 500, and 560 K are shown in Figures 3 through 5. These graphs are plots of the concentration of hydrazine reacted against the concentration of hydrazine remaining on a log-log basis. The order of the reaction is given by the slope and the rate is given by the intercept. In all cases, the order is definitely less than one, even allowing for experimental scatter; most of the data are well represented by a 3/4-order line.

Figure 4 shows data obtained at 560 K over a tenfold concentration range with each aperture and a total concentration range of thirtyfold. It can be seen that over this entire range, the order is constant at 3/4. Figure 5 shows a similar behavior at 472 K over the same concentration range. These figures also show the effect of leaving the activated catalyst under vacuum ($\sim 10^{-8}$ torr) for varying periods of time at different temperatures. The rate of vacuum poisoning seems to increase with temperature, thus lowering the rate of reaction; the order remains the same at $\sim 3/4$.

C. Experiments Using Powdered Catalyst

Since the orders of reaction measured with pelletized catalyst suggested that the reaction was diffusion controlled, we conducted experiments using a single catalyst pellet that had been gently crushed to a fine

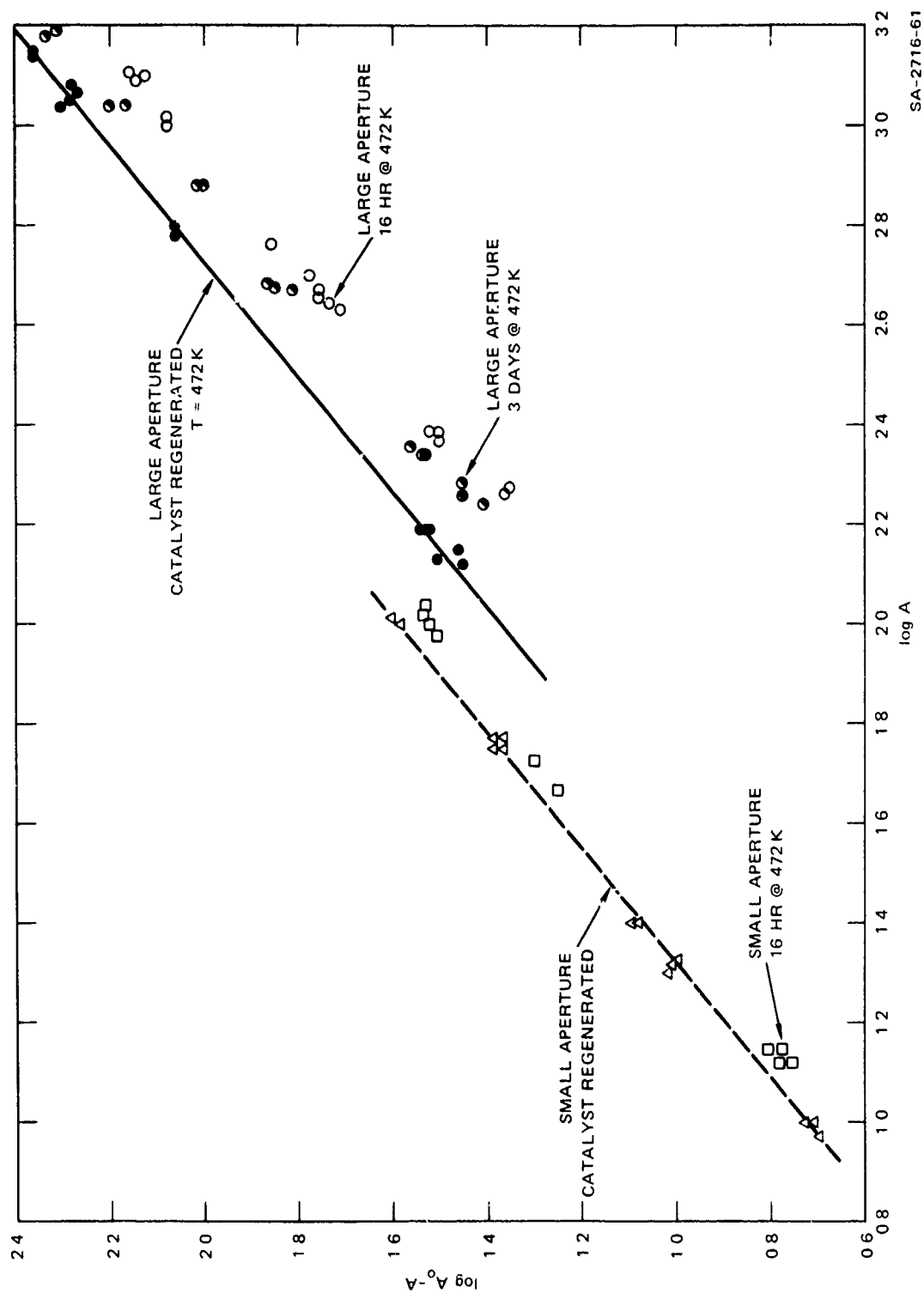


FIGURE 3 PLOT OF LOG [CONCENTRATION OF HYDRAZINE DECOMPOSED] AGAINST LOG [CONCENTRATION OF HYDRAZINE REMAINING]

A_0 = Concentration of hydrazine with no reaction, A = concentration of hydrazine with reaction occurring.
At 472 K on pelletized catalyst

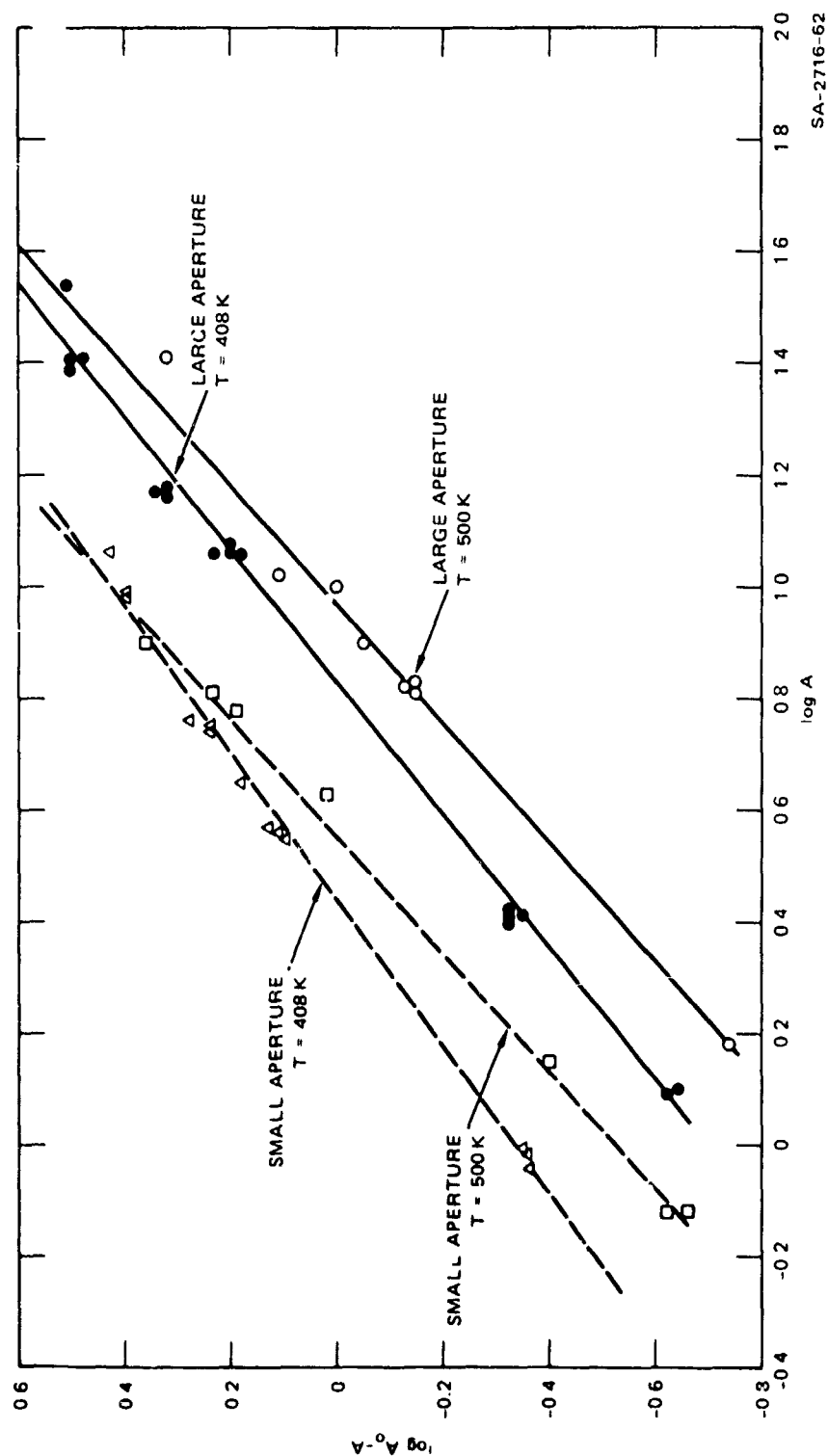


FIGURE 4 PLOT OF LOG [CONCENTRATION OF HYDRAZINE DECOMPOSED] AGAINST LOG [CONCENTRATION OF HYDRAZINE REMAINING]

A_0 = Concentration of hydrazine with no reaction, A = concentration of hydrazine with reaction occurring. At 408 and 500 K on pelletized catalyst.

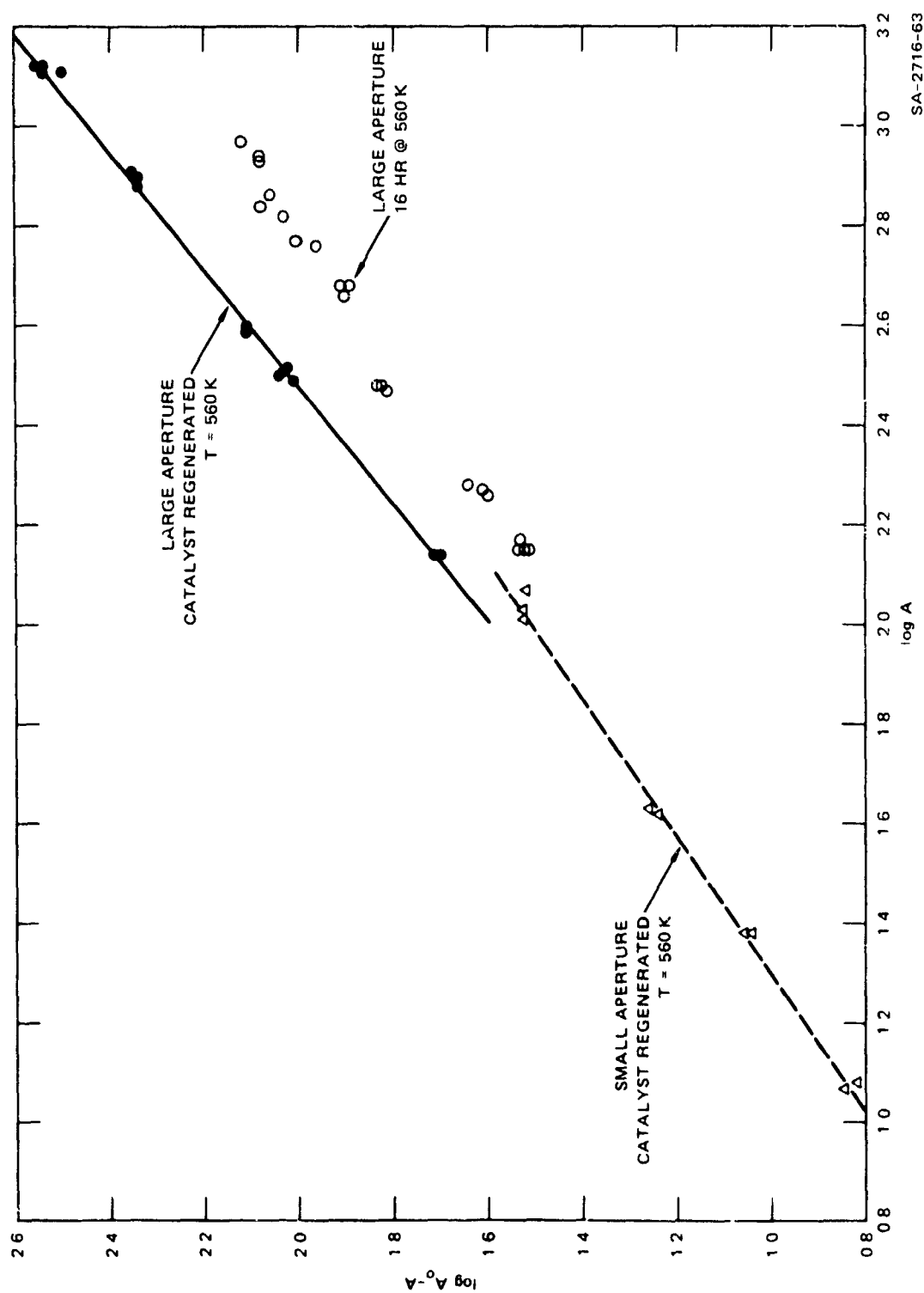


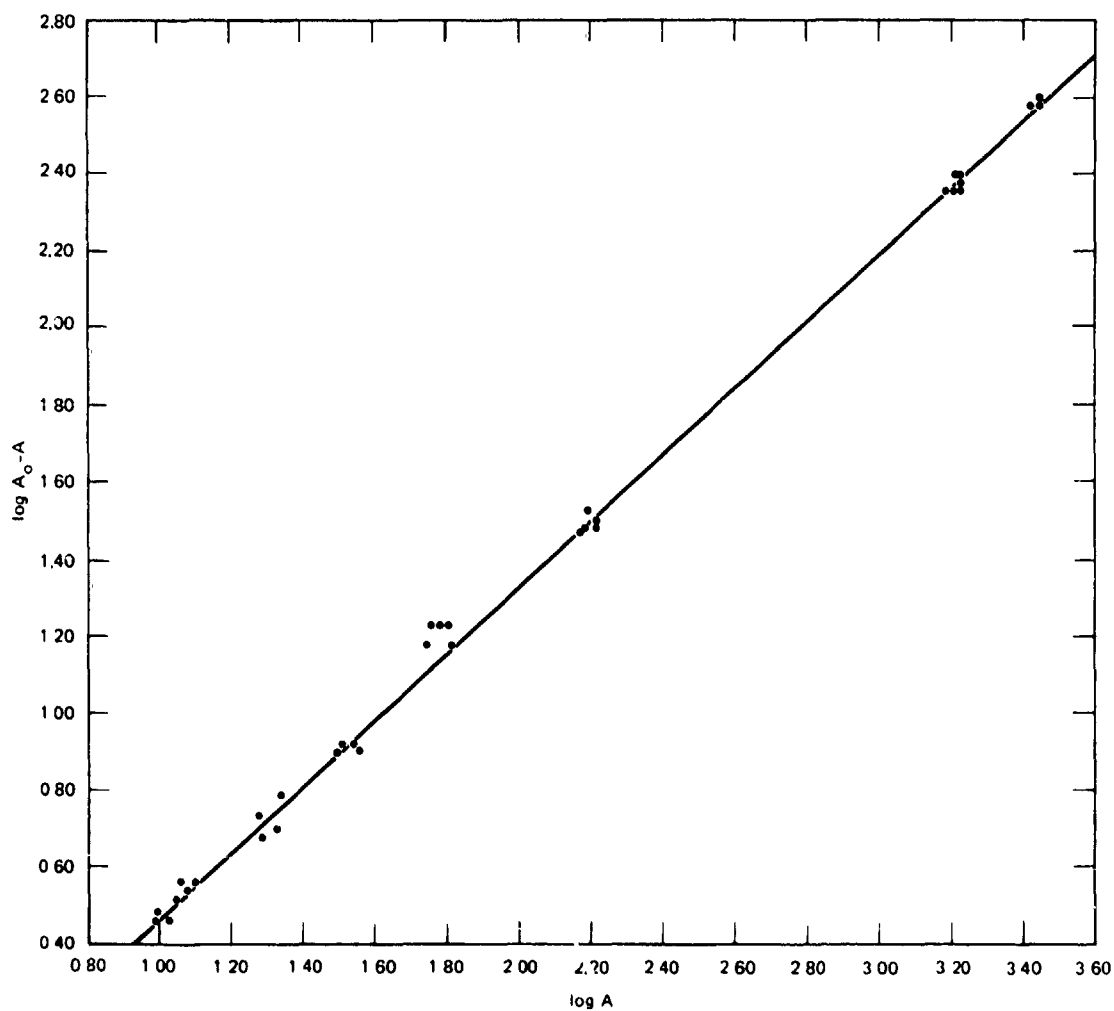
FIGURE 5 PLOT OF LOG [CONCENTRATION OF HYDRAZINE DECOMPOSED] AGAINST LOG [CONCENTRATION OF HYDRAZINE REMAINING]

A_0 = Concentration of hydrazine with no reaction, A = concentration of hydrazine with reaction occurring
At 560 K on pelletized catalyst

powder. This gave rates of decomposition comparable to those from five pellets, owing to the greater surface area exposed. The results of these experiments are plotted in Figures 6* and 7. The results at 485 and 549 K show that over an extremely wide concentration range (~ 100 -fold), the order is constant and best fit by a 9/10 line. The concentration range is sufficient to enable us to verify that a first-order line will not fit the results.

Although the reaction is not first order, first-order rate constants can justifiably be calculated and used to determine the temperature dependence of the rate constant in a single experiment. The catalyst was activated in the normal way, and then allowed to cool to the reaction temperature under vacuum. Then, using a constant flow of hydrazine, we measured the rate of decomposition while varying the temperature continuously. The results are plotted in Arrhenius form in Figures 8 and 9; that is, log percentage reaction (proportional to the first-order decomposition rate constant) is plotted against reciprocal temperature. Figure 8 shows the effect of heating and cooling. The experiment began at high temperature ($1/T = 1.6 \times 10^{-3}$), and the reactor was then cooled down to room temperature and subsequently heated. We believe the results obtained under cooling are more accurate because the whole reactor is in thermal equilibrium. Under heating conditions, the heating coils are considerably hotter than the reaction vessel, and the measured temperature could be higher than the real temperature, producing the effect that is seen.

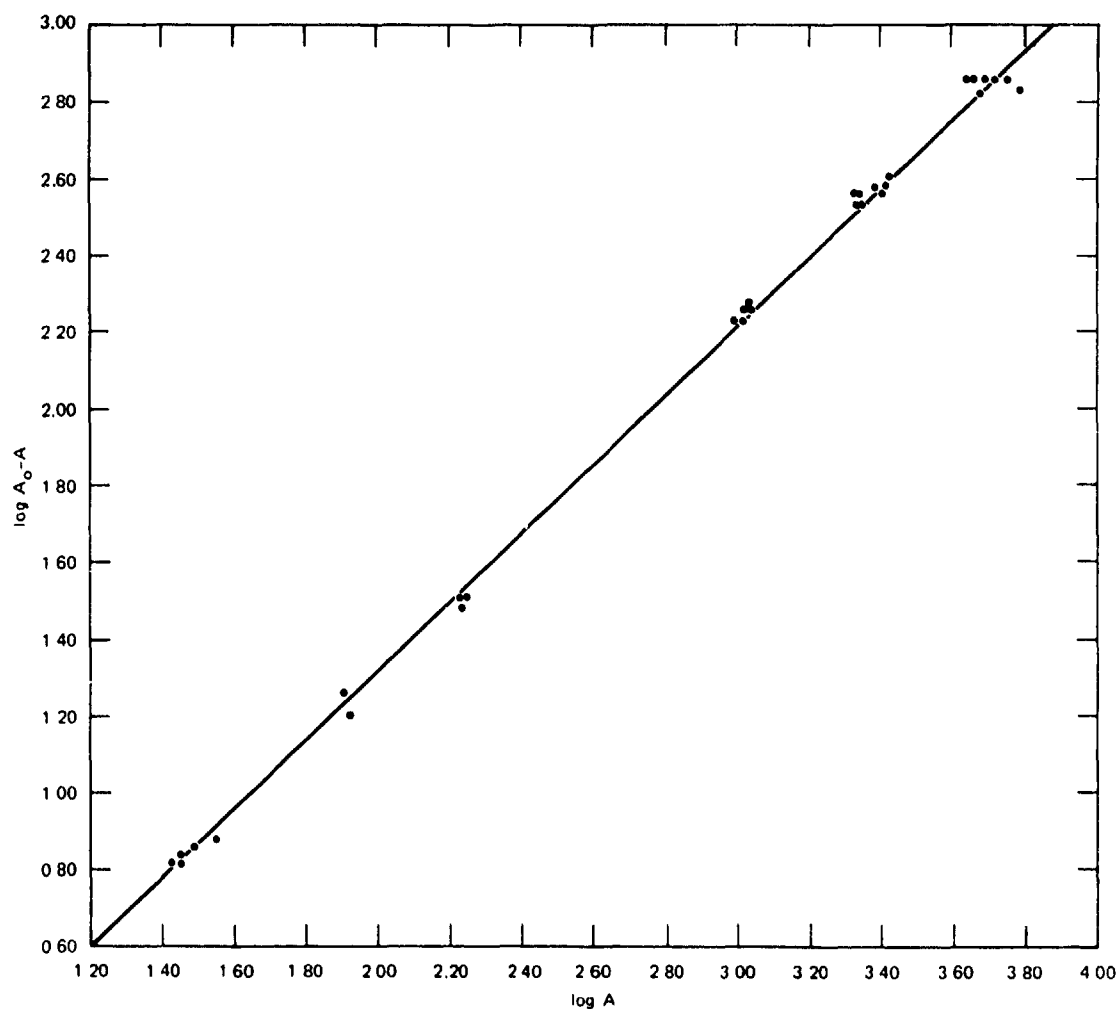
* Detailed data for this and subsequent figures are given in the Appendix, Tables A-1 through A-5.



SA-2716-64

FIGURE 6 PLOT OF LOG [CONCENTRATION OF HYDRAZINE DECOMPOSED] AGAINST LOG [CONCENTRATION OF HYDRAZINE REMAINING]

A_0 = Concentration of hydrazine with no reaction, A = concentration of hydrazine with reaction occurring. At 485 K on powdered catalyst.



SA-2716 65

FIGURE 7 PLOT OF LOG [CONCENTRATION OF HYDRAZINE DECOMPOSED] AGAINST LOG [CONCENTRATION OF HYDRAZINE REMAINING]

A_0 = Concentration of hydrazine with no reaction, A = concentration of hydrazine with reaction occurring. At 549 K on powdered catalyst

Comparison of Figures 8 and 9 shows a wide discrepancy between the measured activation energies; the difference in absolute values of the fractional reaction is to be expected for different aperture sizes. The measured activation energy should be constant. These results reflect the irreproducibility of the catalyst activity referred to earlier, even though the same catalyst and treatment were used in both cases. Figure 9 shows linear Arrhenius behavior over a temperature range from 380 to 770 K.

D. Products of the Reaction

We have made a brief study of the products of the reaction on the powdered catalyst sample. The results are shown in Figure 10, where spectral signal intensities are plotted against temperature. Note that the relative magnitude of the signals for different species is not proportional to their relative concentrations due to differing mass spectral sensitivities. As shown, the product distribution changes significantly over the range from 400 to 850 K.

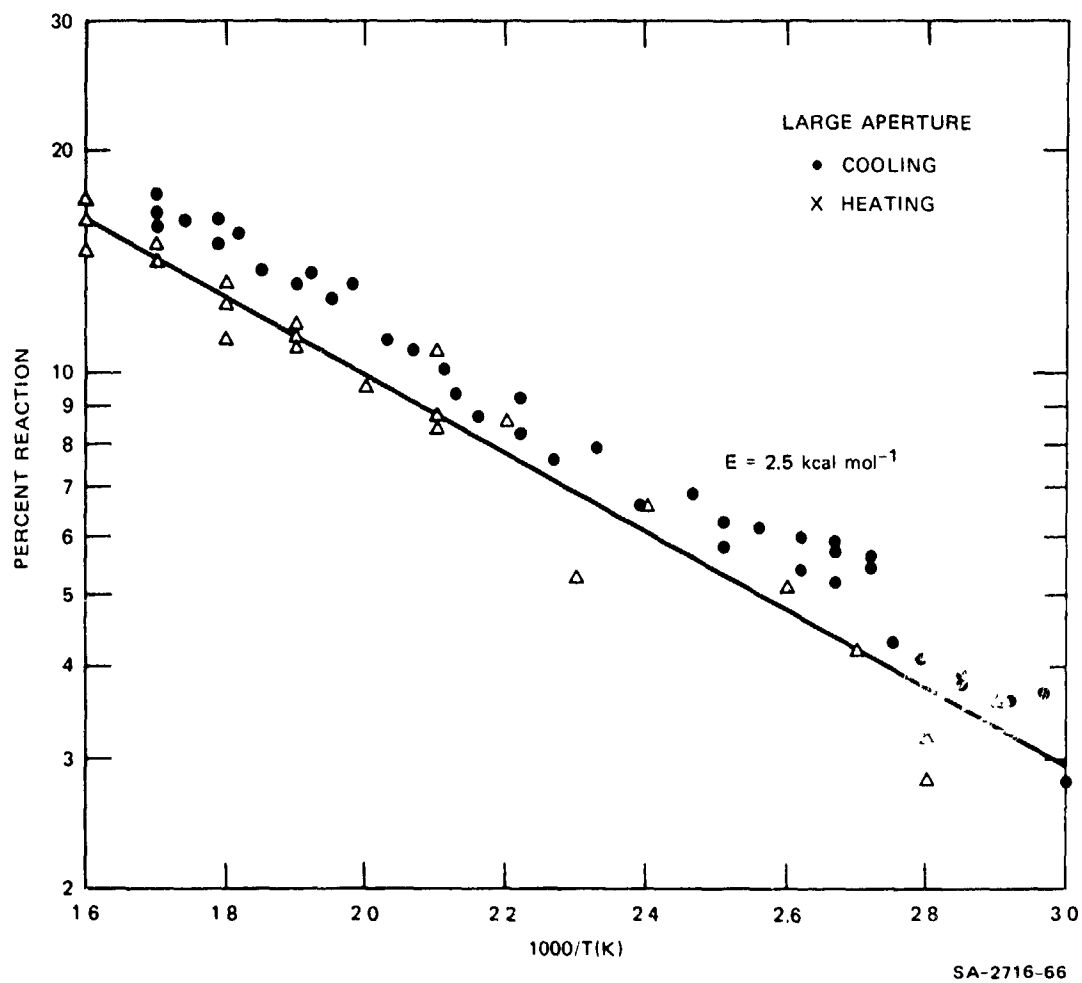
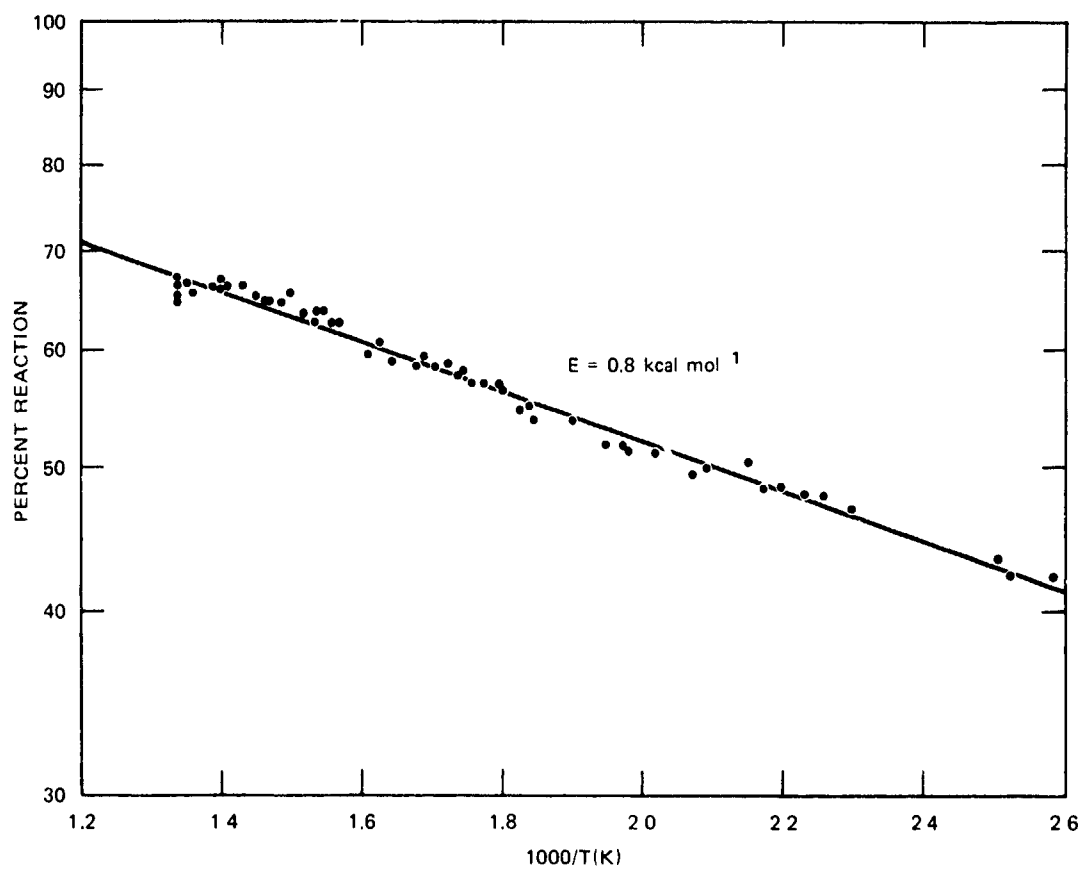


FIGURE 8 ARRHENIUS PLOT OF THE DECOMPOSITION OF HYDRAZINE ON POWDERED CATALYST

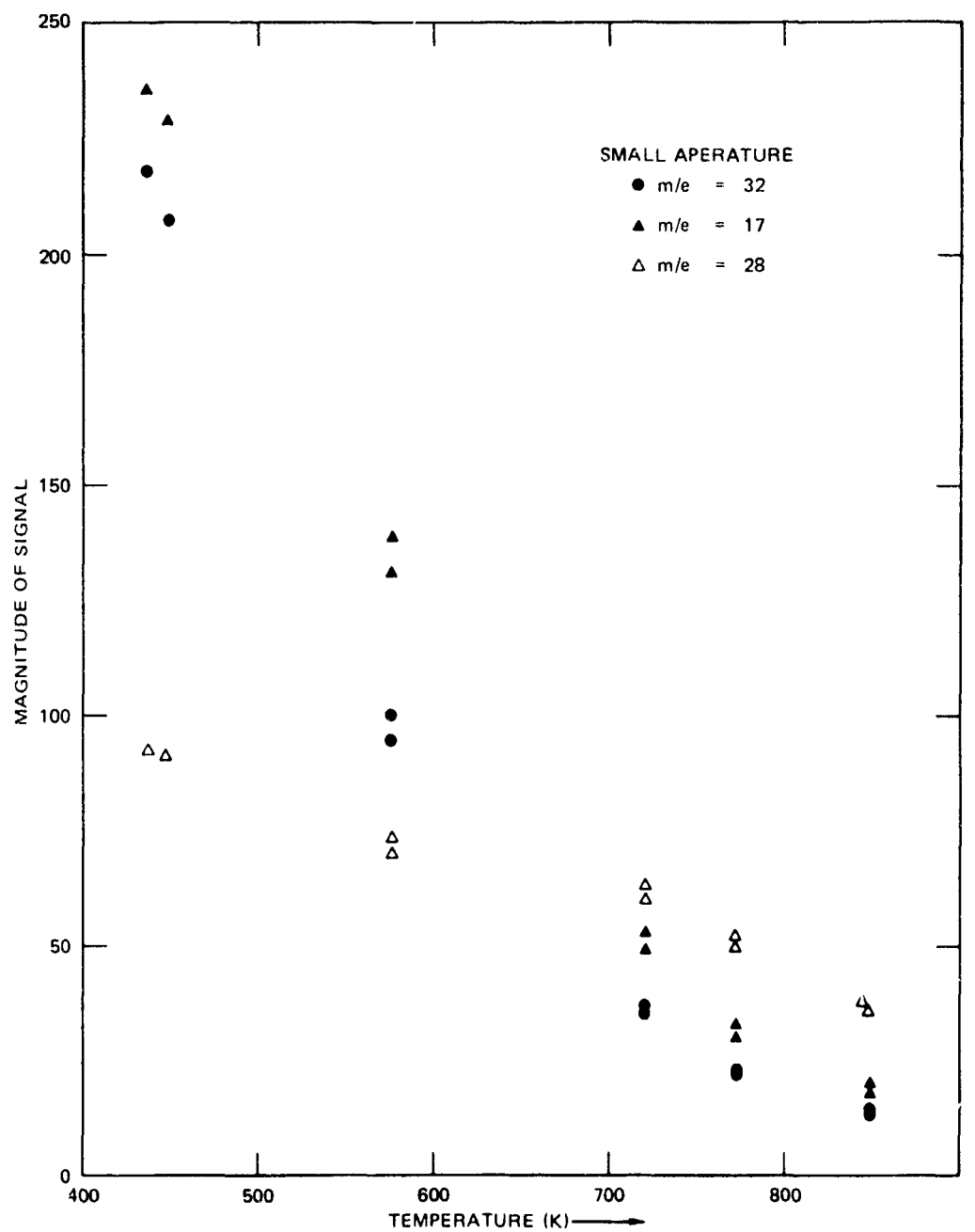
Percent reaction is proportional to the first-order rate constant.



SA-2716-67

FIGURE 9 ARRHENIUS PLOT OF THE DECOMPOSITION OF HYDRAZINE ON POWDERED CATALYST

Percent reaction is proportional to the first-order rate constant.



SA-2716-68

FIGURE 10 PRODUCT DISTRIBUTION AS A FUNCTION OF TEMPERATURE

IV. DISCUSSION

In attempting to investigate more completely the results of the decomposition of hydrazine on Shell-405 that were reported last year, we have discovered that experimental artifacts play a much larger part than was previously realized. The principal problem is that activated catalyst under high-vacuum ($\sim 10^{-8}$ torr) experiences a decline in activity, presumably because of surface poisoning by residual gases. This means that the catalyst must be activated immediately before every experiment. Unfortunately, there seems to be a large irreproducibility involved in the activation process. Use of a completely standardized activation procedure on the same catalyst can yield widely varying results in consecutive experiments. We have been unable to relate this effect to any physical parameter of the system. Hence, previous results may have been influenced by these experimental artifacts.

One problem in comparing experiments at different temperatures is that a standard procedure cannot be followed. Activation of the catalyst takes place at 100 K; cooling from this high temperature takes a significant time (~ 3 hours to room temperature), and cooling to different reaction temperatures takes differing periods of time. Thus, the catalyst presumably experiences a differing amount of vacuum poisoning, depending on the temperature. Previous experiments on the temperature dependence of the reaction where different experiments were conducted at different temperatures are almost certainly unreliable. In particular, we can find no minimum in reactivity around 450 K. All of our Arrhenius plots show good linearity over the range 300 to 770 K (Figures 8 and 9). These plots do show differing activation energies that presumably reflect

the fact that the experiments were begun at different temperatures, or possibly just a general irreproducibility.

Examination of Figure 8 shows that, as previously reported,⁷ the product distribution changes at ~ 600 K. Above 600 K, much less ammonia is produced, with a corresponding increase in nitrogen and hydrogen. However, there seems to be no change of rate at this temperature. This strongly suggests that the rate-limiting step is nonchemical; it is unlikely that a change in the mechanism of decomposition would not result in a change of rate if the rate-limiting step were chemical.

The above conclusion is supported by the low measured values of the activation energy, which are characteristic of diffusion-controlled reactions.⁹ Diffusion control would also explain the nonintegral orders of reaction observed. Our measurements show that over an extremely wide range of concentration and temperature, the order of the reaction is constant and definitely less than one. On pelletized catalyst, the order is best represented by a 0.75 line and on powdered catalyst by a 0.9 line. The increase in order observed when a powdered catalyst is used presumably reflects a lessening of the influence of pore diffusion; on powdered catalyst, the reaction probably takes place mainly on the exposed surface.

In conclusion, our study has reemphasized the extreme difficulties and need for caution in conducting experiments at low pressures with very active catalysts. Experimental problems in handling the catalyst have precluded the investigation of the detailed mechanism of decomposition of hydrazine on Shell-405. To achieve this, it would be necessary to conduct experiments in a regime where diffusion was fast relative to chemical reaction, and under conditions rigorously designed to prevent catalyst poisoning.

It is unfortunate that while the VLPP technique has demonstrated its ability to accurately measure the rate of heterogeneous reactions, the results have been rendered inconclusive by problems of surface sensitivity. It will thus be necessary to use UHV conditions to fully realize the potential of VLPP in heterogeneous reactions.

REFERENCES

1. B. J. Wood and H. Wise, J. Cat., 39, 471 (1975).
2. J. L. Falconer and H. Wise, J. Cat., 43, 220 (1976).
3. A. E. Bucher, W. F. Brinkman, J. P. Maitu, and A. J. Cooper, Phys. Rev., B1, 274 (1970).
4. D. W. Bassett and H. W. Habgood, J. Phys. Chem., 64, 769 (1960).
5. W. A. Blanton, C. H. Byers, and R. P. Merrill, I and E C Fundamentals, 7, 611 (1968).
6. M. Suzuki and J. M. Smith, Chem. Eng. Sci., 26, 221 (1971).
7. D. M. Golden, K. E. Lewis, R. T. Rewick, S. E. Stein, and H. Wise, SRI Annual Report to AFOSR on Contract F44620-73-C-0069, September 1976.
8. S. W. Benson, D. M. Golden and G. N. Spokes, Angew. Chem. (Intnat. Edit.), 12, 534 (1973).
9. C. N. Satterfield and T. K. Sherwood, The Role of Diffusion in Catalysis, Addison Wesley (Reading, Mass.), 1963.

Appendix to Section 2

DATA FOR FIGURES 6 through 10

Table A-1
DATA FOR FIGURE 6*

Sensitivity	A ₀	A	Δ	%	log A	log A ₀ -A
0.02 x 10 ⁻⁹	12.7	9.8	2.9	22.8	0.99	0.46
	13.0	10.0	3.0	23.1	1.00	0.48
	13.5	10.6	2.9	21.5	1.03	0.46
	14.5	11.2	3.3	22.8	1.05	0.52
	15.4	12.0	3.4	22.1	1.08	0.53
	39.0	31.6	8.0	20.2	1.50	0.90
	40.6	32.2	8.4	20.7	1.51	0.92
	43.8	34.4	9.4	21.5	1.54	0.92
	44.6	36.4	8.2	18.4	1.56	0.91
	190	156	34	17.9	2.19	1.53
	174	162	32	16.5	2.21	1.51
	194	162	32	16.5	2.21	1.51
	192	162	30	15.6	2.21	1.48
	182	152	30	16.5	2.18	1.48
	182	152	30	16.5	2.18	1.48
	182	152	30	16.5	2.18	1.48
	1910	1660	250	13.1	3.22	2.40
	1910	1600	250	13.1	3.22	2.40
	1900	1670	230	12.1	3.22	2.36
	1890	1650	240	12.7	3.22	2.38
	1900	1650	250	13.2	3.22	2.40
	3040	2660	380	12.5	3.42	2.58
	3140	2740	400	12.7	3.44	2.60
	3140	2760	380	12.1	3.44	2.58
	3140	2740	400	12.7	3.44	2.60
	3120	2740	380	12.2	3.44	2.58
	70	55	15	21.4	1.74	1.18
	74	57	17	23.0	1.76	1.23
	77	60	17	22.1	1.78	1.23
	78	61	17	21.8	1.79	1.23
	80	65	15	18.8	1.81	1.18
	15.1	11.5	3.6	23.8	1.06	0.56
	16.3	12.7	3.6	22.1	1.10	0.56

continued...

Table A-1 (concluded)

Sensitivity	A_0	A	Δ	%	log A	log $A_0 - A$
	24.4	10.0	5.4	22.1	1.28	0.73
	24.6	19.2	5.4	22.0	1.28	0.73
	24.4	19.6	4.8	19.7	1.29	0.68
	26.2	21.2	5.0	19.1	1.33	0.70
	28.0	21.8	6.2	22.1	1.34	0.79
	1860	1610	250	13.4	3.21	2.40
	1880	1640	240	12.8	3.21	2.38
	1830	1600	230	12.6	3.20	2.36
	1800	1570	230	12.8	3.20	2.36
	1760	1530	230	13.1	3.18	2.36

* Experimental conditions: one Shell-405 pellet, crushed and reactivated by exposure to H_2 at 1000 K; $T = 212^\circ C$ (485 K); date of experiment, 4-26-77.

Table A-2
DATA FOR FIGURE 7*

Sensitivity	A ₀	A	Δ	%	log A	log A ₀ -A
0.02 x 10 ⁻⁹	6720	6040	680	10.1	3.78	2.83
	6420	5520	720	11.5	3.75	2.86
	5880	5160	720	12.2	3.71	2.86
	5520	4800	720	13.0	3.68	2.86
	5360	4680	680	12.7	3.67	2.83
	5200	4480	720	13.8	3.65	2.86
	5120	4400	720	14.1	3.64	2.86
	5080	4360	720	14.20	3.64	2.86
	2540	2200	340	13.4	3.34	2.53
	2520	2180	340	13.5	3.34	2.53
	2520	2160	360	14.3	3.33	2.56
	2520	2160	340	14.3	3.33	2.56
	2500	2160	340	13.6	3.33	2.53
	2520	2160	360	14.3	3.33	2.56
	1140	970	170	14.9	2.99	2.23
	1190	1020	170	14.3	3.01	2.23
	1230	1050	180	14.6	3.02	2.26
	1250	1060	190	15.2	3.03	2.28
	1260	1070	190	15.1	3.03	2.28
	1270	1090	180	14.2	3.04	2.26
	100	82	18	18.0	1.91	1.26
	100	82	18	18.0	1.91	1.26
	100	84	16	16.0	1.92	1.20
	33.6	27.0	6.6	19.6	1.43	0.82
	35.0	28.2	6.8	19.4	1.45	0.83
	38.0	30.8	7.2	18.9	1.49	0.86
	43.4	35.8	7.6	17.5	1.55	0.88
	3020	2620	400	13.2	3.42	2.60
	2940	2560	380	12.9	3.41	2.58
	2900	2400	500	13.1	3.38	2.58
	2860	2500	360	12.5	3.40	2.56
	202	170	32	15.8	2.23	1.51
	204	174	30	14.7	2.24	1.48
	208	176	32	15.4	2.25	1.51

Experimental conditions: large aperture; one Shell-405 pellet, crushed and reactivated by exposure to H₂ at 1000 K; T = 276°C (549 K).

Table A-3
DATA FOR FIGURE 8*

Temp (K)	A ₀	A	Δ	% Rxn
587	176	148	28	15.9
587	177	151	26	14.7
587	180	150	30	16.7
587	183	151	32	17.5
575	186	156	30	16.1
559.5	182	155	27	14.8
	184	154	30	16.3
550	187	158	29	15.5
541	188	162	26	13.8
	194	164	30	15.5
527	182	158	24	13.2
520	182	157	25	13.7
512	182	159	23	12.6
504	189	164	25	13.2
492	190	169	21	11.1
484	195	174	21	10.8
475	199	179	20	10.1
470	171	155	16	9.4
462	171	156	15	8.8
451	174	158	16	9.2
	180	165	15	8.3
440	184	170	14	7.6
429	164	151	13	7.9
418	182	170	12	6.6
405	189	176	13	6.9
398	189	178	11	5.8
	192	180	12	6.3
390	195	183	12	6.2
381	166	157	9	5.4
	168	158	10	6.0
375	170	160	10	5.9
375	171	161	10	5.8
	173	164	9	5.2
367	177	167	10	5.6

continued...

Table A-3 (concluded)

Temp (K)	A ₀	A	Δ	% Rxn
367	181	171	10	5.5
363.5	187	179	8	4.3
358	191	183	10	4.1
351	205	197	8	3.9
	209	201	8	3.8
343	224	216	8	3.6
	215	207	8	3.7
337	212	206	6	2.8
333	216	210	6	2.8
293	213	209	4	1.9
	219	206	3	1.4
315	225	223	2	0.9
340	220	212	8	3.6
352	217	210	7	3.2
359	215	209	6	2.8
367	215	206	9	4.2
379	216	205	11	5.1
409	226	211	15	6.6
429	208	197	11	5.3
	199	189	10	5.0
461	194	181	17	8.6
475	188	172	16	8.5
487	183	167	16	8.7
500	178	161	17	9.6
506	178	159	19	10.7
516	175	156	19	10.9
521	173	153	20	11.6
532	170	151	19	11.2
538	169	150	19	11.2
544	169	150	19	11.2
	168	147	21	12.5
566	165	143	22	13.3
579	163	140	23	14.1
593	160	136	24	15.0
609	155	132	23	14.8
626	153	128	25	16.3
637	150	124	26	17.3

Experimental conditions: large aperture; one Shell-405 pellet, crushed and reactivated by exposure to H₂ at 1000 K; date of experiment, 5-4-77.

Table A-4
DATA FOR FIGURE 9*

Temp (°C, K)	A ₀	A	Δ	σ%	1000/K
748 K	97	34	63	64.9	1.337
475 = 748	92	32	60	65.2	
475 = 748	92	31	61	66.3	
475 = 748	92	31	61	66.3	
475 = 748	92	31	61	66.3	
475 = 748	92	30	62	67.4	
471 = 744	94	31	63	67.0	
467 = 740	95	32	63	66.3	1.351
462 = 735	96	33	63	65.6	1.361
447 = 720	101	34	67	66.3	1.389
444 = 717	103	35	68	66.0	1.395
441 = 714	106	35	71	67.0	1.401
438 = 711	109	37	72	66.1	1.406
435 = 708	110	37	73	66.4	1.412
427 = 700	116	39	77	66.4	1.429
423 = 696	118	40	78	66.1	1.437
415 = 688	121	42	79	65.3	1.453
411 = 684	125	44	81	64.8	1.462
408 = 681	131	46	85	64.9	1.468
401 = 674	136	48	88	64.7	1.484
396 = 669	142	49	93	65.5	1.495
387 = 660	150	55	95	63.3	1.515
384 = 651	152	55	97	63.8	1.536
379 = 652	159	59	100	62.9	1.534
374 = 647	166	61	105	63.3	1.546
369 = 642	171	64	107	62.6	1.558
365 = 638	179	67	112	62.6	1.567
349 = 622	204	83	121	59.3	1.608
342 = 615	220	86	134	60.9	1.626
336 = 609	229	94	135	59.0	1.642
324 = 597	256	106	150	58.6	1.675
319 = 592	268	108	160	59.7	1.689
314 = 587	274	114	160	58.4	1.704
308 = 581	282	116	166	58.9	1.721

continued...

Table A-4 (concluded)

Temp ($^{\circ}\text{C}$, K)	A_0	A	Δ	%	1000/K
304 = 577 K	288	122	166	57.6	1.733
300 = 573	296	124	172	58.1	1.745
296 = 569	302	130	172	57.0	1.757
291 = 564	308	132	176	57.1	1.773
285 = 558	316	136	180	57.0	1.792
283 = 556	322	140	182	56.5	1.799
275 = 548	336	152	184	54.8	1.825
272 = 545	342	154	188	35.0	1.835
268 = 541	346	160	186	53.8	1.848
253 = 526	364	168	196	53.8	1.901
240 = 513	398	192	206	51.8	1.949
234 = 507	412	198	214	51.9	1.972
232 = 505	420	204	216	51.4	1.980
222 = 496	444	216	228	51.4	2.076
210 = 483	470	238	232	49.4	2.070
205 = 478	490	245	245	50.0	2.092
193 = 466	505	250	255	50.5	2.146
188 = 461	515	265	250	48.5	2.169
182 = 455	525	270	255	48.6	2.198
175 = 448	530	275	255	48.1	2.232
170 = 443	535	280	255	47.7	2.257
162 = 435	555	295	260	46.8	2.299
126 = 399	645	365	280	43.4	2.505
123 = 396	650	375	275	42.3	2.525
114 = 387	675	390	285	42.2	2.584

* Experimental conditions: small aperture; one Shell-405 pellet, crushed and reactivated by exposure to H_2 at 1000 K; date of experiment, 7-14-77.

Table A-5
DATA FOR FIGURE 10*

Temp (K)	m/e = 14	15	16	17	28	29	30	31	32	
840	18	23	106	111	184	27	25	45	70	s = 0.10
	16.8	18.0			175.9	2.63	1.88	0	0	
840	18	26	114	120	193	27	26	49	72	s = 0.10
	16.9	20.6	96.3	99.4	184.4	2.71	2.29	3.29	0	
773	12	18	89	94	134	20	18	36	56	s = 0.05
	10.7	14.0	75.2	77.8	127.9	0	0	0	0	
773	14	20	95	98	135	21	19	36	56	s = 0.05
	13	16.1	80.8	82.0	129.1	0	0	0	0	
718	17	30	138	148	161	32	30	56	88	s = 0.05
	15	22	116	123	151	0	0	0	0	
718	18	33	150	157	166	32	30	57	92	s = 0.05
	16	27	127	132	156	0	0	0	0	
578	10	32	149	156	78	33	31	58	95	s = 0.02
	9	26	128	131	70	0	0	0	0	
578	11	34	157	165	83	34	32	60	100	s = 0.02
	9	27	135	139	73	0	0	0	0	
448	16	60	268	280	110	72	66	122	208	s = 0.02
	13	47	224	229	91	0	0	0	0	
438	7	30	138	144	55	37	34	63	109	s = 0.01
	6	23	115	118	46	0	0	0	0	

NOTE: First row of figures for each temperatures is raw data.

Second row is data corrected for N₂H₄ cracking pattern.

* Experimental conditions: small aperture; one Shell-405 pellet, crushed and reactivated by exposure to H₂ at 1000 K; date of experiment, 7-15-77.